Chalcogenide Letters Vol. 8, No. 3, March 2011, p. 177 – 185

PREPARATION AND CHARACTERIZATION OF CdS NANOPARTICLES BY CHEMICAL CO-PRECIPITATION TECHNIQUE

B.SRINIVASA RAO[a], B.RAJESH KUMAR[b*], V.RAJAGOPAL REDDY[a], T.SUBBA RAO[b]
[a]*Department of Physics, Sri Venkateswara University, Tirupati-517502, A.P, India*
[b]*Department of Physics, Sri Krishnadevaraya University, Anantapur-515055, A.P, India*

In the present work, conventional chemical co-precipitation method was employed for the preparation of CdS nanoparticles. XRD studies reveal that CdS crystallizes in single phase hexagonal structure. The particle size of CdS nanoparticles is obtained as 13nm. Microstructural analysis using Scanning Electron Microscope (SEM) supplemented with EDAX were carried out for the sample to find grain size as well as chemical composition. SEM study reveals that the sample consist of nanoclusters, the grains have aggregated to form clusters. A detailed systematic study on CdS sample is done by characterizing TEM, UV-VIS-NIR spectra, Photoluminescence (PL) spectra, DSC/TGA and FTIR.

(Received March 14, 2011, accepted March 24, 2011)

Keywords: CdS, Nanoparticles, X-ray diffraction, Transmission Electron Microscopy, Optical band gap, Photoluminescence spectra

1. Introduction

Nanostructure sulfides and selenides (e.g.CdSe, ZnSe, CdS and ZnS) have been extensively studied with a view to establish a relationship between structure, size and optical properties [1]. II-VI semiconductor nanoparticles are currently of great interest for their practical applications such as zero-dimensional quantum confined materials in optoelectronics and photonics. Among these, CdS has been studied due to its potential technological applications in field effect transistors, solar cells, photovoltaic, light emitting diodes, photocatalysis, photoluminesce, infrared photodetector, environmental sensors and biological sensors [2-8]. There are various methods reported in the literature to fabricate nanoparticles by physical [9,10], chemical methods [11] and ion implantation [12]. In the present study we have synthesized CdS nanoparticles through chemical co-precipitation technique. CdS nanoparticles are extensively characterized using XRD, HRSEM with EDX, TEM, UV-VIS-NIR spectrophotometer, DSC/ TGA, Photoluminescence (PL) spectra and FTIR spectroscopy.

2. Experimental

CdS nanoparticles are prepared by the colloidal chemical precipitation method using cadmium acetate ($CdCH_3COOH$), sodium sulfide (Na_2S) as starting compounds and using thiophenol as capping agent. These compounds are weighed in a microbalance (M/s SICO, India). The stoichiometric solution was taken in a burette and was added in drops with continuous sitting to precipitate of CdS was formed. After complete precipitation, the solution in conical flask was

* Corresponding author: rajphyind@gmail.com

constantly stirred for about 20 hours. Then the precipitates were filtered out. The samples were calcined at 300°C/2hrs in vacuum. The structure and phase of the sample are determined by X-ray diffraction using Bruker X-ray diffractometer and using CuK_α (λ =0.15406nm) radiation. X-ray diffraction (XRD) measurements have been performed by using Bruker AXS D8 advance model PW 1600, powder X-ray diffractometer using CuK_α (λ =0.15406nm) has been used as the source of X-rays. Surface Morphology of the sample has been studied using FEI Quanta FEG 200 High Resolution Scanning Electron Microscope (HRSEM) with energy dispersive X-ray spectrometry (EDX). Bright Field Transmission Electron Microscopy (TEM) image and Selected Area Electron Diffraction (SAED) pattern of the sample are performed on Philips CM 120 ST transmission electron microscope operated at 100 kV, with Å resolution. Diffraction patterns have been recorded over the range of $20^o - 75^o$ at the scan rate of 2^o/min. Differential scanning calorimetry (DSC) and Thermo gravimetric Analysis (TGA) curves were recorded for the sample using Perkin Elmer SDT 600 with a heating rate of 20^o/min in the temperature range RT-700°C. Fourier transform infrared (FT-IR) measurements were carried out using Perkin Elmer Spectrum1 FT-IR. IR spectra of fine powdered samples were obtained in a KBr pellet in the range 400-4000cm^{-1} with a resolution of 4cm^{-1}. UV-visible spectrum of the nanoparticles is recorded using Cary 5E UV-VIS-NIR spectrophotometer in the wavelength range 190-800 nm. Photoluminescence spectra of the sample are recorded using Jobin Yvon Fluorolog-3-11 spectroflurometer from the range 180-850nm.

3. Results and discussions

Figure 1 shows X-ray diffraction pattern of CdS. The patterns can be assigned to hexagonal cadmium sulfide phase by comparing with the standard data from JCPDS card (File No. 41-1049). The six main diffraction peaks are corresponding to (0 0 2), (1 0 0), (1 0 1), (1 1 0), (1 0 3) and (1 1 2) planes respectively, similar results found in Balram Tripathi et al [13]. The lattice parameters for CdS hexagonal system is found to be a=4.143A°, b=4.143A° and c=6.719A°. From the Full Width at Half Maximum(FWHM) of the most intense peak particle size has been calculated by using the Scherer formula[14], $D=0.9\lambda/\beta\cos\theta$, where λ is the wavelength of X-ray diffraction, β is FWHM in radians of the XRD peak and θ is the angle of diffraction. The particle size of the sample is found to be 13nm. The peaks from XRD have been indexed with the help of a computer program – POWDIN [15] using the observed interplanar spacing d. Table 1 shows the observed and calculated values computed from Powdin Program.

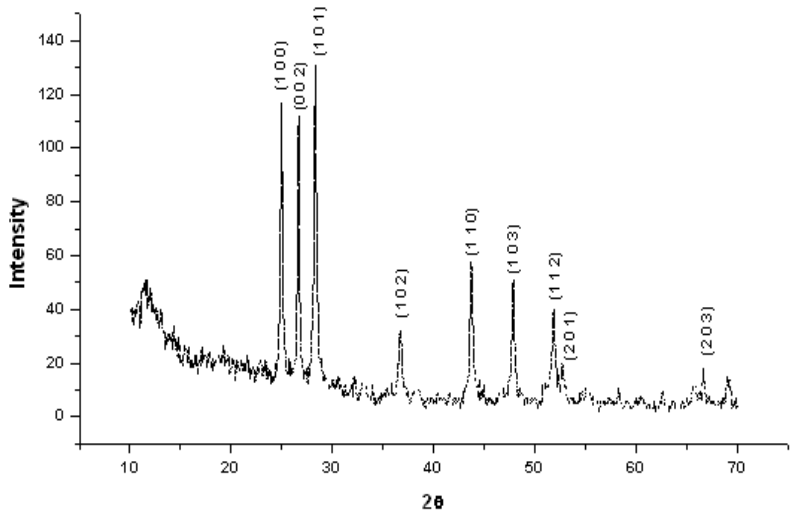

Fig. 1. XRD pattern for CdS sample

Table 1. Observed and calculated values of interplanar spacing (d) and miller indices (h k l) from Powdin Program.

Lattice Parameters, a= 4.143A^0, c= 6.719 A^0, c/a= 1.4914; Volume, V= 99.73 $(A^0)^3$

Line o.	c.	d-spacing A. obs.	calc.	Indices h	k	l	SinSqTheta*E4 obs.	calc.	2Theta Deg. obs.	calc.	diff
1	1	3.5649	3.5853	1	0	0	466.8	461.5	24.96	24.81	.145
2	2	3.3447	3.3595	0	0	2	530.3	525.7	26.63	26.51	.119
3	3	3.1497	3.1632	1	0	1	598.0	593.0	28.31	28.19	.123
4	4	2.4470	2.4515	1	0	2	990.8	987.2	36.69	36.63	.069
5	5	2.0691	2.0700	1	1	0	1385.9	1384.6	43.71	43.69	.021
6	6	1.8989	1.8995	1	0	3	1645.4	1644.3	47.86	47.85	.017
7	8	1.7620	1.7623	1	1	2	1911.1	1910.3	51.85	51.83	.011
8	9	1.7345	1.7321	2	0	1	1972.0	1977.6	52.73	52.81	-.081
9	10	1.6638	1.6797	0	0	4	2143.3	2102.7	55.16	54.59	.569
10	11	1.5842	1.5816	2	0	2	2363.9	2371.8	58.18	58.29	-.107
11	12	1.4799	1.5211	1	0	4	2708.9	2564.2	62.73	60.85	1.881
12	13	1.4027	1.3996	2	0	3	3015.2	3028.9	66.61	66.78	-.171
13	14	1.3583	1.3551	2	1	0	3215.6	3230.8	69.09	69.28	-.186

The SEM image shown in figure 2 with different magnifications clearly indicates the formation of nanoclusters. The grains have aggregated to form clusters [16]. Figure 3 shows the clear peaks of Cadmium (Cd) and Sulphur (S), compositional analysis by EDAX confirms that the sample is around the nominal composition. EDAX data shown in Table 2 gives the compositions of prepared sample in weight percentage.

Table 2. EDAX data for CdS

Compound Name	Element	Weight Percentage (%)
CdS	S K	47.23
	Cd L	52.77
		Total 100.00

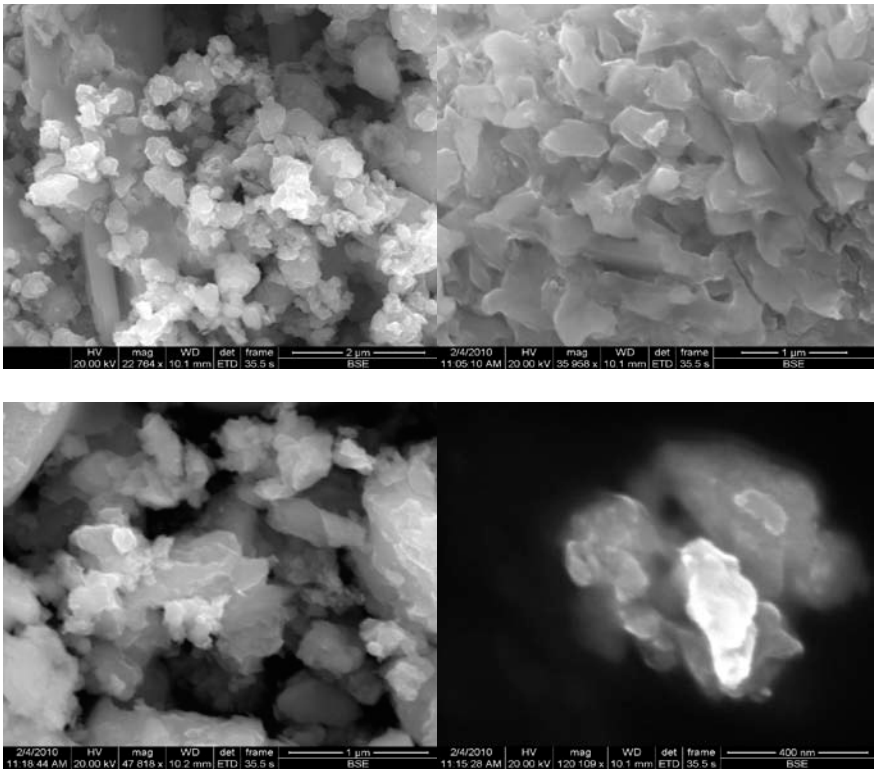

Fig. 2. SEM of CdS with different magnifications

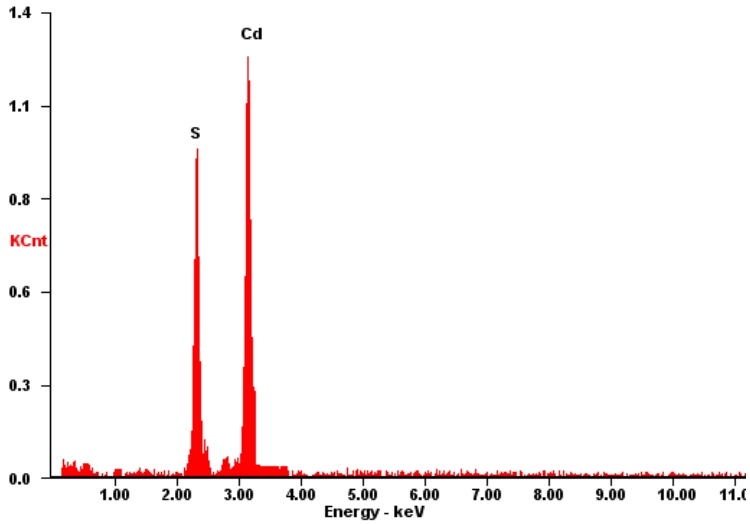

Fig. 3. EDAX plot of CdS

In order to examine the structure of prepared sample selected area electron diffraction (SAED) patterns and diffraction contrast images were taken. Typical SAED from representative CdS sample is shown in figure 4. Figure 5 depicts the Bright Field TEM micrographs of CdS. The cadmium sulfide was obtained as uniform and fine particles, which form crystalline aggregates. From TEM studies, the calculated lattice parameters a=4.138A^{o}, b=4.138A^{o} and c=6.692A^{o} and

particle size of 12 nm was found to be in good agreement with the values reported from the XRD data.

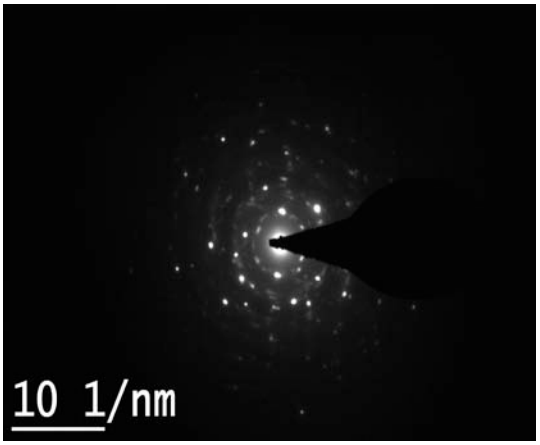

Fig. 4. Selected area Electron Diffraction (SAED) pattern of CdS

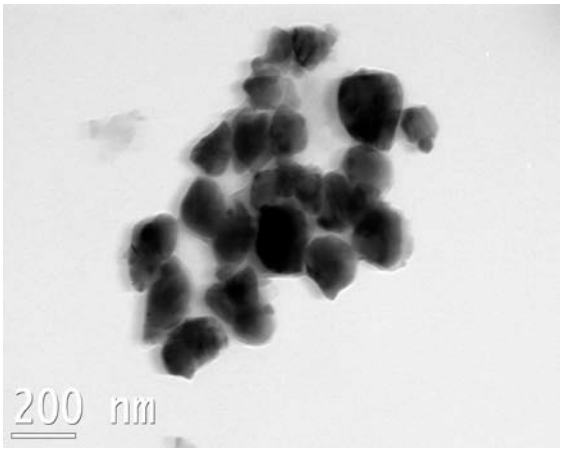

Fig. 5. Bright Field TEM image of CdS

The most dramatic property of semiconductor nanoparticles is the size evolution of optical absorption spectra. Hence UV-visible absorption spectroscopy is an efficient technique to monitor the optical properties of quantum-sized particles. Figure 6 shows optical absorption spectra of CdS. The bulk band gap of CdS is 2.42eV, as reported by earlier workers [17]. In the present work optical band gap is calculated using the Tauc relation [18, 19]. Tauc relation is described as

$$(\alpha h\nu)^{1/n} = A(h\nu - E_g) \quad (1)$$

Where A is a constant and E_g is the band gap of the materials and exponent n depends on the type of transition. For direct allowed transition n=1/2, indirect allowed transition n=2, direct forbidden transition n=3/2 and forbidden indirect transition n=3 [20]. To determine the possible transitions, $(\alpha h\nu)^2$ vs hν is plotted and corresponding band gap were obtained from extrapolating the straight portion of the graph on hν axis. The direct band gap values of the sample have been obtained from $(\alpha h\nu)^2$ vs plot as shown in the figure 7. The direct band gap value of sample is found to be 3.7eV, this value is shifted compared with the bulk value and this could be a consequence of a size quantization effect in the sample. The reduction in particle size gives a shift in the optical band gap of the sample. Since the band gap increases as the particle size is reduced, the emission wavelength shifts towards higher energies (lower wavelengths). The UV-visible spectrum in

figure 4 shows that the onset of absorption for the sample is ~516nm. Realising that our CdS nanoparticles sample may not be strictly monodispersed, the fine structure on the higher energy side of the broad green emission may be assigned as band-edge emissions from particles of different sizes.

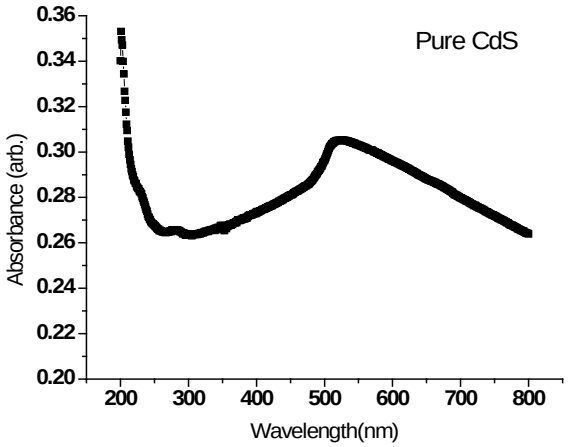

Fig. 6. Optical absorption spectra of CdS

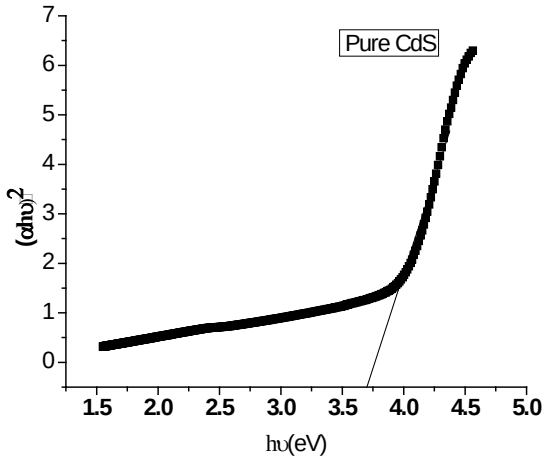

Fig. 7. Determination of Band gap of CdS

In literature various models related to the size confinement effect (SCE) were reported. A simple model was initially adapted by Efros [21] in 1982 to spherical clusters with infinite potential walls as boundary conditions. These authors assumed an energy dispersion close to the valence band maximum (VBM) and the conduction band minimum (CBM) with effective masses of CBM electron and VBM hole. This model is called the "effective mass approximation" (EMA). A further development of the EMA model has been made by Brus[22]. The latter has introduced the Coloumb interaction, leading to the following equation:

$$E_g^{nano} - E_g^{bulk} = h^2/8r^2\,(1/m_e^* + 1/m_h^*) - 1.8e^2/4\Pi\varepsilon_0\varepsilon_r - 0.248\,E^*_{Ry} \qquad (2)$$

where E_g^{nano} and E_g^{bulk} are the respective nanoparticles and bulk energy gaps, r is the radius of the particle, m_e^* & m_h^* are the reduced masses of the conduction band electron and valence band hole in units of electron mass, h is Planck's constant, ε_0 is the vacuum permittivity, ε is the high-frequency dielectric constant, E^*_{Ry} is effect Rydberg energy given by

$$E^*_{Ry} = e^4/2\varepsilon^2h^2\,(1/m_e^* + 1/m_h^*)^{-1} \qquad (3)$$

The average nanoparticle diameter calculated from the absorption spectra by means of quantum confinement theory is 2.52nm for CdS.

The photoluminescence originates from the recombination of surface states [23]. The strong PL implies that the surface states remain very shallow, as it is reported that quantum yields of band edge will decrease exponentially with increasing depth of surface state energy levels [24]. Fig. 8 shows the Photoluminescence (PL) spectrum of CdS nanoparticles with excitation wavelength 328nm and the PL peak is about 410nm. The luminescence from the surface states (around 800nm) has also been observed. The peak of eigen-transition is strong and steep; the emission peak of surface states is flat and weak. The PL full-width half-maximum (fwhm) is only about 30nm, it reveals that the narrow size distribution of nanoparticles. Photoluminescence analysis in 400-650 nm emission wavelengths shows the 'well known' green emission band in CdS nanoparticle.

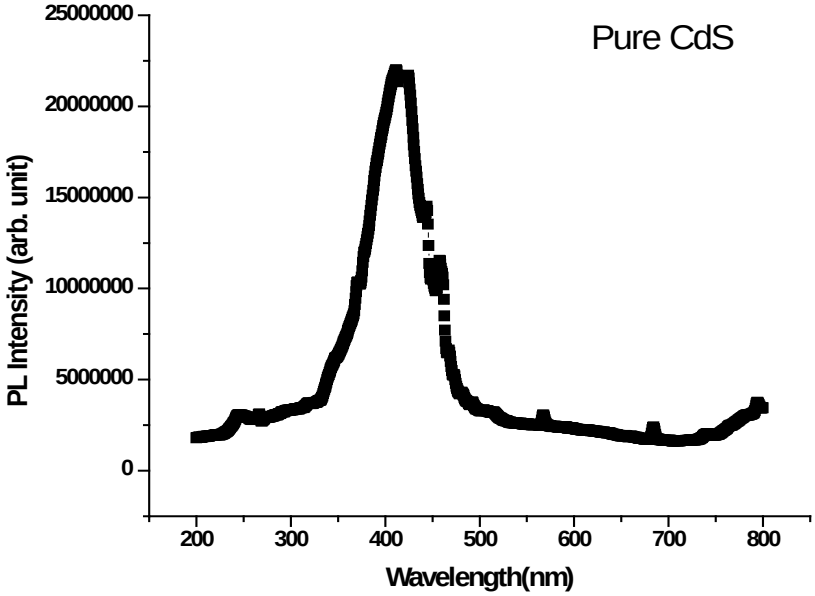

Fig. 8. Photoluminescence spectra of CdS

Thermo gravimetric Analysis (TGA) trace of CdS from 50 -700^{o}C is shown in figure 9. There is a weight loss from 420^{o}C to 500^{o}C due to loss of absorbed water on the surface of materials. It is followed by a major weight loss up to 600^{o}C and is ascribed to decomposition of covalently bound organic, particularly thiophenol on the surface. Differential Scanning Calorimetry (DSC) trace of CdS derived between 50 -700^{o}C is shown in figure 10. There is an intense exothermic peak between 420^{o}C to 500^{o}C coinciding with weight loss in its TGA trace as shown in figure 9. It is due to desorption of water from the surface of the nanoparticles. The exothermic peak lying between 420^{o}C to 500^{o}C is due to decomposition and desorption of thiophenol.

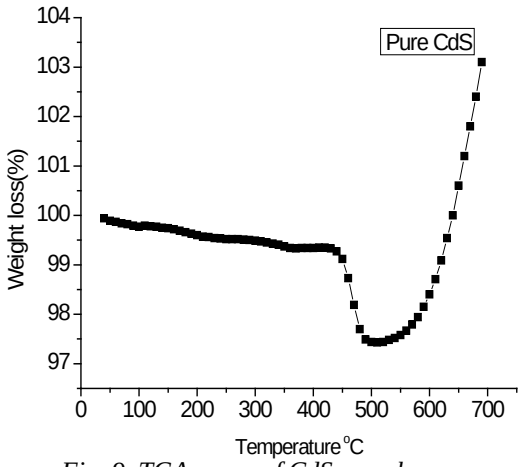

Fig. 9. TGA curve of CdS sample

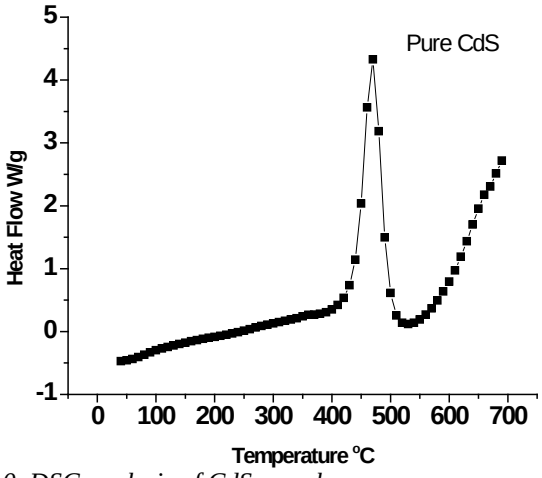

Fig. 10. DSC analysis of CdS sample

The FTIR spectrum of pure CdS is shown in figure 11. In the higher energy region the peak at 3420cm^{-1} is assigned to O-H stretching of absorbed water on the surface of CdS. The presence of water is confirmed by its bending vibration at 1625 cm^{-1}. The peak at 1425 is assigned to bending vibration of methanol used in the process. It is also verified by its CH_3-stretching vibrations occurring as very weak peaks just below 3000 cm^{-1}. The C-O stretching vibration of absorbed methanol gives its intense peak at 1098 cm^{-1}. The weak peaks due to C-H stretching are observed at about 618cm^{-1}. Hence in addition to absorbed methanol on the surface of CdS, presence of thiophenol in its dissociation form is also evident. These observations convincingly support template role of thiophenol in the control of the size of CdS particles.

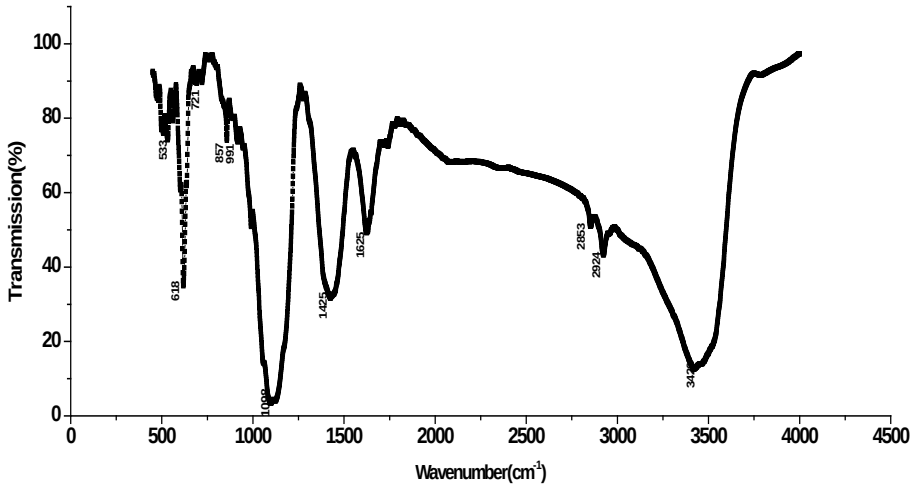

Fig.11. FTIR spectra of CdS sample

4. Conclusion

CdS nanoparticles have been synthesized by aqueous medium through chemical co-precipitation technique. X-ray diffraction measurement confirms the structure, single phase hexagonal and particle size (13nm) of the sample. TEM studies of CdS obtained as uniform and fine particles, which form crystalline aggregates. From optical absorption measurements it is found that the band gap increases while the wavelength of absorbance onset shifts to shorter wavelengths. Therefore, the onset wavelength is directly related to nanoparticle size. From PL spectra, the position of emission peak shifts towards higher energy with the decrease of nanoparticles size

References

[1] V.I. Klimov, J. Phys. Chem. B **110**, 16827(2006).
[2] A.Fukoka, Y.Sakamoto, S.Guan, S.Inagaki. N.Sugimoto, Y.Fukushima, K.Hirahara, S.Iijima, M.Ichikawa, J.Am.Chem.Soc. **123**, 3373(2001).
[3] A.Henglein, Chem.Rev.89, 1861(1989).
[4] C.Petit, M.P.Pilleni, J.Phys.Chem. **92**, 2282(1988).
[5] A.P.Alivisatos, Science **271**, 933 (1996).
[6] V.L.Kolvin, M.C.Schlamp, A.P.Ailivisatos, Nature **370**, 354(1994).
[7] D.L. Klein, R.Roth, A.K.L. Lim, A.P.Ailivisatos, Nature **389**, 699(1997).
[8] C.Yang, X.Zhou, L.Wang, X.Tian, Y.Wang, Z.Pi, J.Mater.Sci. **44**,3015(2009).
[9] F.Antolini, A.Ghezelbash, C.Esposito, E.Trave, L.Tapfer, B.A.Korge, Mater.Letter. **60**, 1095(2006).

[10] J.S.Jie, W.J.Zhang, Y.Jiang, X.M.Meng, Y.Q.Li, S.T.Lee, Nano Lett. **6**, 1887(2006).
[11] N.V.Deshmukh, T.M.Bhave, A.S.Ethiraj, S.R.Sainkar, V.Ganesan, S.V.Bhoraskar, S.K.Kulkarni, Nanotechnology **12**,290-294(2001).
[12] U.V.Denisca, O.Gamulin, A.Tonej, M.Ivanda, C.W.White, E.Sonder, R.A.Zuhr, Mater.Sci.Eng.C **15**,105(2001).
[13] Balram Tripathi, Y.K.Vijay, F.Sing, D.K.Avasthi, S.Wate, Journal of Alloys and Compounds **459**, 118(2008).
[14] B.D Cullity, Elements of X-Ray Diffraction, Addison-Wesley, Reading, MA, (1977).
[15] E.Wu, POWD, An interactive powder diffraction data interpretation and indexing program Ver2.1, School of Physical Science, Flinders University of South Australia, Bedford Park S.A. 5O42 AU.
[16] M.Thambidurai, N.Muthukumarasamy, S.Agilan, N.Murugan, N.Sabari Arul, S.Vasantha and R. Balasundaraprabhu, Solid State Sciences **12**, 1554-1559 (2010).
[17] L.E.Brus, J.Chem.Phys.**79**, 5566(1983).
[18] J.Tauc (Ed.), Amorphous and Liquid Semiconductors, Plenum Press, New York, 159 (1974).
[19] C.W.Litton, D.C.Reynolds, Phys.Rev. A **133**, 536 (1964).
[20] J.I.Pankove, Optical Process in Semiconductors, New Jersey, USA 34 (1971).
[21] A.I.Efros, A.L.Efros, Sov.Phys.Semicond. **16**,772 (1982).
[22] L.E.Brus, J.Chem.Phys.**90**, 2555(1986).
[23] N. Chestony, T.D. Harris, R. Hull L.E. Brus, J**.** Phys**.** Chem**. 90,** 3393 (1986).
[24] R. J. Heath, J. J. Shiang, Chem**.** Soc**.** Rev**. 27**, 65 (1998).